Hindawi Publishing Corporation
Indian Journal of Materials Science
Volume 2015, Article ID 927364, 8 pages
http://dx.doi.org/10.1155/2015/927364

Research Article

Structural, Optical, Electrical, and Magnetic Properties of PVA:Gd^{3+} and PVA:Ho^{3+} Polymer Films

M. Obula Reddy[1,2] and B. Chandra Babu[2]

[1]*Department of Physics, Loyola Degree College, Pulivendula 5163902, India*
[2]*Department of Physics, Sri Venkateswara University, Tirupati 517502, India*

Correspondence should be addressed to B. Chandra Babu; chandrababuphd@gmail.com

Received 17 February 2015; Accepted 17 April 2015

Academic Editor: Amir Kajbafvala

Polymer films of PVA:Gd^{3+} and PVA:Ho^{3+} have been synthesized by a solution casting method in order to study their structural, optical, electrical, and magnetic properties. The semicrystalline nature of the polymer films has been confirmed from XRD analysis. The FTIR analysis confirms the complex formation of the polymer with the metal ions. Dielectric studies of these films have also been carried out at various set temperatures in the frequency from 100 Hz to 1 MHz for carrying out impedance spectroscopy analysis to evaluate the electrical conductivity which arises due to a single conduction mechanism and thus to have a single semicircle pattern from these polymer films. The DC electrical conductivity increases with an increase in the temperature and it could be due to high mobility of free charges (polarons and free ions) at higher temperatures. The conductivity trend follows the Arrhenius equation for PVA:Gd^{3+} and for PVA:Ho^{3+} polymer films. PVA:Gd^{3+} polymer films show ferromagnetic nature, and PVA:Ho^{3+} polymer films have revealed paramagnetic nature based on the trends noticed in the magnetic characteristic profiles.

1. Introduction

In recent years energy conversion devices based on organic semiconductors are an emerging research field with substantial future prospects and it has attracted great attention due to the advantages of light weight, flexibility, and low cost of production with the possibility of fabricating large area devices based on solution processing. Polymeric materials have been the subject of intense scientific and technological research because of their potential applications. In particular, conducting polymers have been extensively investigated in the area of electronics and optoelectronics due to their attractive properties [1, 2]. Polymeric dielectric materials have been preferred because of their dielectric and physical properties over a wide range of temperatures and frequencies. Over the years, among various polymers, poly(vinyl alcohol) (PVA), as one of the most important polymers, has recently received considerable interest, owing to its numerous potential applications in electronic components. It has different internal structure that may be considered as amorphous or semicrystalline. The semicrystalline structure of PVA showed an important feature rather than of amorphous one. This is because semicrystalline PVA leads to formation of both crystalline and amorphous regions [3–5].

PVA polymer is soluble in water and other solvents and is widely used in synthetic fiber, paper, contact lens, textile, coating, and binder industries, due to its excellent chemical and physical properties, nontoxicity, processability, good chemical resistance, high dielectric strength, good charge storage capacity, wide range of crystallinity, good film formation capacity, complete biodegradability, and high crystal modulus dopant-dependent electrical and optical properties [6–9]. PVA is comprised of carbon chain backbone with hydroxyl groups attached to methane carbons; these OH groups can be a source of hydrogen bonding and hence assist in the formation of polymer composite. Interestingly, semicrystalline materials have exhibited improvement in certain physical properties due to crystal-amorphous interfacial effect [9].

The rare earth elements will exhibit ferromagnetism in addition to the unique luminescent nature. Luminescence from the RE^{3+} ions originates from the transitions between 4f orbitals, and these transitions are forbidden on symmetry grounds [10–12]. Among various rare earth activated systems, gadolinium and holmium materials emerged as promising candidates for such applications. In the present work, we prepared and characterized the PVA polymer with gadolinium Gd^{3+} ($4f^7$) and holmium Ho^{3+}($4f^{10}$) doping polymer films considered to investigate the features of optical, dielectric, and magnetic studies. Hence, these polymer films may be used in electrochemical display systems.

2. Experimental Studies

2.1. Sample Preparation. Spectral pure host matrix chemical of polyvinyl alcohol (PVA) (with MW = 1, 30,000) and dopant chemicals of $GdCl_3{\cdot}6H_2O$ and $HoCl_3{\cdot}6H_2O$ were used in the present work. Development of transparent PVA:Gd^{3+} and PVA:Ho^{3+} polymer films was done for obtaining Gd^{3+}:PVA and Ho^{3+}:PVA films upon gadolinium chloride/holmium chloride by using the solution casting method. Both the host polymer and dopant chemicals were dissolved separately in double distilled water (DDW) in the proportion of 1 : 9 and such mixed solutions were stirred thoroughly using a magnetic stirrer at temperature 60°C for 12 hrs and thus the homogenously mixed solution was poured on to Petri dish for obtaining transparent polymer films through slow evaporation method after 48 hrs from those dishes, and those neatly formed transparent polymer films were collected into appropriate containers for measurement purposes. All the obtained polymer films were in 150 μm thickness in good transparencies. These prepared PVA:$Gd^{3+}$and PVA:Ho^{3+} polymer films were cut into 2 cm × 1 cm sizes for undertaking the experimental studies on them.

2.2. Characterization Techniques. The structures of the prepared polymers were characterized on XRD 3003 TT Seifert diffractometer with Cuk_α radiation (λ = 1.5406 Å) at 40 KV and 20 mA and the 2θ range between 10° and 70°. Perkin-Elmer FT-IR spectrophotometer was used for recording FT-IR spectra of the host PVA, and the doped PVA:Gd^{3+} and PVA:Ho^{3+} polymer films in the region of 4000–400 cm^{-1}. The absorption spectra of the above prepared films were measured on Varian-Cary-Win. Spectrometer (JASCO V-570), and both excitation and emission spectra of these polymer films were recorded on a SPEX FLUOROLOG (model-II) attached with a Xe-arc lamp (150 W). Dielectric measurements carried out using Phase Sensitive Multimeter (PSM) (Model-1700). The magnetic moment profile as function of applied magnetic field was measured on a Vibratory Sample Magnetometer with a range of ±20 KOer.

3. Results and Discussion

3.1. XRD Analysis. The XRD patterns of the host matrix PVA and 10 wt% of Gd^{3+} and Ho^{3+}:PVA polymer films are shown in Figures 1(a)–1(c). The XRD pattern of pure PVA shows a characteristic peak at $2\theta \approx 19.8^0$ which confirms the semicrystalline nature of orthorhombic structure. Even after the doping of La^{3+} ion by Gd^{3+} and Ho^{3+} ion the matrix semicrystalline nature does not change, but intensity of the peak decreases gradually, suggesting a decrease in the degree of crystallinity of PVA. They observed that the intensity of XRD peak decreases as the amorphous nature increases with the addition of dopant [13, 14].

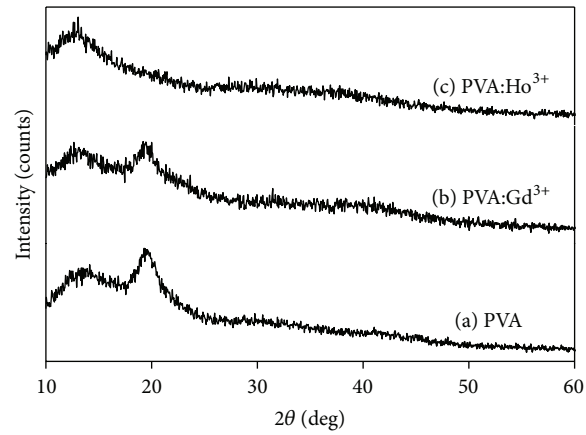

Figure 1: (a–c) XRD profiles of PVA, PVA:Gd^{3+}, and PVA:Ho^{3+} polymer films.

3.2. FTIR Analysis. Figures 2(a)–2(c) show an FTIR spectra pure PVA and 10 wt% of Gd^{3+} and Ho^{3+}:PVA polymers. All the spectra exhibit the characteristic bands of virgin PVA which are stretching and bending vibrations of O-H, C-O, C=C, and C-H groups. Abroad and strong band is observed at 3333 cm^{-1} which arises from (OH) stretching frequency and indicates the presence of hydroxyl group and 2940 cm^{-1} corresponds to the anti-symmetric. A weak band observed at 2168 cm^{-1} has been attributed to the combination frequencies of the rocking and the stretching vibrations. A moderate absorption peaks at 1730 cm^{-1} and 1655 cm^{-1} have been attributed to the C=O, C=C stretching mode. The FT-IR data along with the band assignments [15, 16] are presented in Table 1. From spectra, it can be noticed that the doping with Gd^{3+} and Ho^{3+} causes some observable changes in the spectrum of PVA in the range 1000–400 cm^{-1}. It induces some new bands and slight changes in the intensities of some bands. The new bands may be correlated likewise to defects induced by the charge transfer reaction between the polymer chain and the dopant [15–17].

3.3. Optical Properties. Figure 3(a) shows a strong absorption band located at 271 nm ($^8S_{7/2} \rightarrow {}^6I_{7/2}$) besides a weak absorption band at 315 nm ($^8S_{7/2} \rightarrow {}^6P_{7/2}$), respectively [18]; these bands can be ascribed to the 4f-4f intraconfigurational transitions between $^8S_{7/2}$ ground state and $^6P_{7/2}$ and $^6I_{7/2}$. Emission spectrum of this polymer film is shown in Figure 3(b), which demonstrates a sharp line 311 nm ($^6P_{7/2} \rightarrow {}^8S_{7/2}$) and an intense peak at about 324 nm with

Table 1: Assignments of FTIR bands of pure PVA and 10 wt% of Gd^{3+} and Ho^{3+}:PVA polymer films.

Pure PVA (cm^{-1})	Gd^{3+}:PVA (cm^{-1})	Ho^{3+}:PVA (cm^{-1})	Assignment
3101–3524	2813–3573	2873–3560	O-H stretching
1706	1709	1711	C=C stretching
1530	1541	1541	C-H bending
1480	1465	1468	CH_2 bending
1230	1238	1243	CH + OH bending
1115	1118	1125	CO stretching
847	854	856	C-C stretching
668	675	675	O-H wagging
562	565	565	CO bending
489	489	489	C-Cl bending

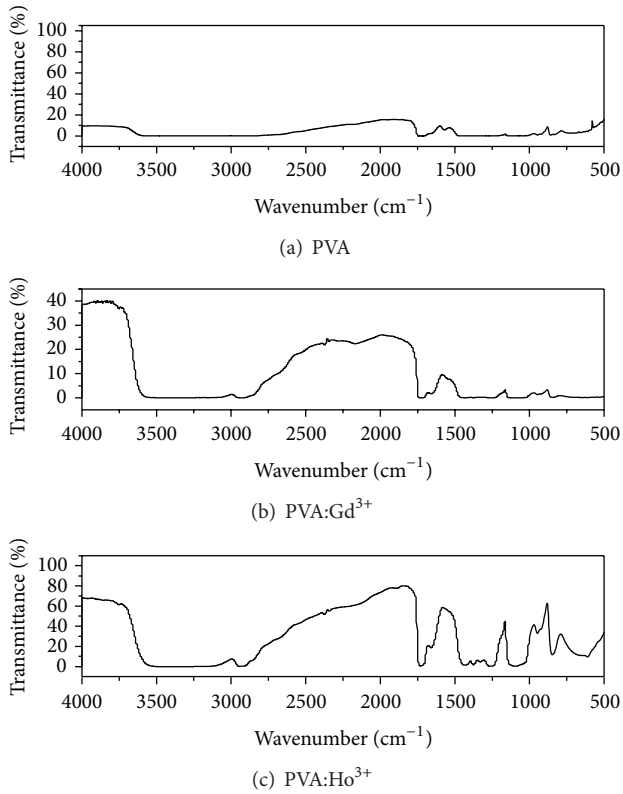

Figure 2: (a–c) FT-IR profile of PVA, PVA:Gd^{3+}, and PVA:Ho^{3+} polymer films.

λ_{exci} = 275 nm [19]. From Figure 4(a), it is observed that there exists a strong absorption band at 380 nm for Ho^{3+}: PVA polymer films besides five weaker absorption bands at 416 nm, 450 nm, 485 nm, 537 nm, and 641 nm respectively, and those have appropriately been assigned to the electronic transitions such as ($^5I_8 \rightarrow {}^5G_4$) at 380 nm, ($^5I_8 \rightarrow (^5G, {}^3G)_5$) at 416 nm, ($^5I_8 \rightarrow {}^5G_5$) at 450 nm, ($^5I_8 \rightarrow {}^5F_3$) at 485 nm, ($^5I_8 \rightarrow {}^5F_4$) at 537 nm, and ($^5I_8 \rightarrow {}^5F_5$) at 641 nm, which are also agreeing with the reported values [20]. From Figure 4(b), a strong blue emission at 433 nm ($^5G_5 \rightarrow {}^5I_8$) can be observed with λ_{exci} = 380 nm and two weak emission bands are observed at 412 nm and 460 nm ($^5G_6 \rightarrow {}^5I_8$), respectively, which are also agreeing with the reported value [21].

3.4. Dielectric Properties. Figures 5(a) and 5(b) show the variation of the dielectric constant (ε') with frequency at different constant temperatures for Gd^{3+}:PVA and Ho^{3+}:PVA polymer films. From the figures, it is clear that the values of the (ε') are very high at low frequency. Such high value of dielectric constant at low frequencies has been explained by the presence of space charge effects, which is contributed by the accumulation of charge carriers near the electrodes. At higher frequencies, dielectric constant has been found to be relatively constant with frequency. This is because periodical reversal of the field takes place so rapidly that the charge carriers will hardly be able to orient themselves in the field direction resulting in the decrease in dielectric constant [22, 23]. The dielectric loss tangent as a function of frequency at various temperatures for Gd^{3+}:PVA and Ho^{3+}:PVA polymer films is shown in Figures 6(a) and 6(b). From the figures, it is clear that the variation of $\tan\delta$ with frequency gives an evidence for a distinct dipolar peak which is temperature dependent. A distribution of molecular weights or cooperation movement of adjacent chains could give the spread of relaxation times. The existence of a peak at relatively lower frequencies is an indication of the longer relaxation time pertinent to polymers composed of macromolecules. It can be seen that as the temperature increases the $\tan\delta$ maximum shifts towards higher frequencies indicating the main dielectric relaxation character of dielectric loss in these polymer films [24].

3.5. Conductivity Analysis. The ionic conductivity of the polymer electrolytes mainly depends on the concentration of conducting dopant and their mobility. The conductivity values can be calculated from the relation $\sigma_{DC} = d/R_bA$, where d is the thickness of the film, A is the area of the film, and R_b is the bulk resistance of the bulk material which is obtained from the intercept of real part of complex impedance plot. Impedance diagrams of PVA: Gd^{3+} and PVA: Ho^{3+} polymer films as shown in Figures 7(a) and 7(b) in temperature range 303–373 K. The plots consist of a high frequency depressed semicircle represented by a

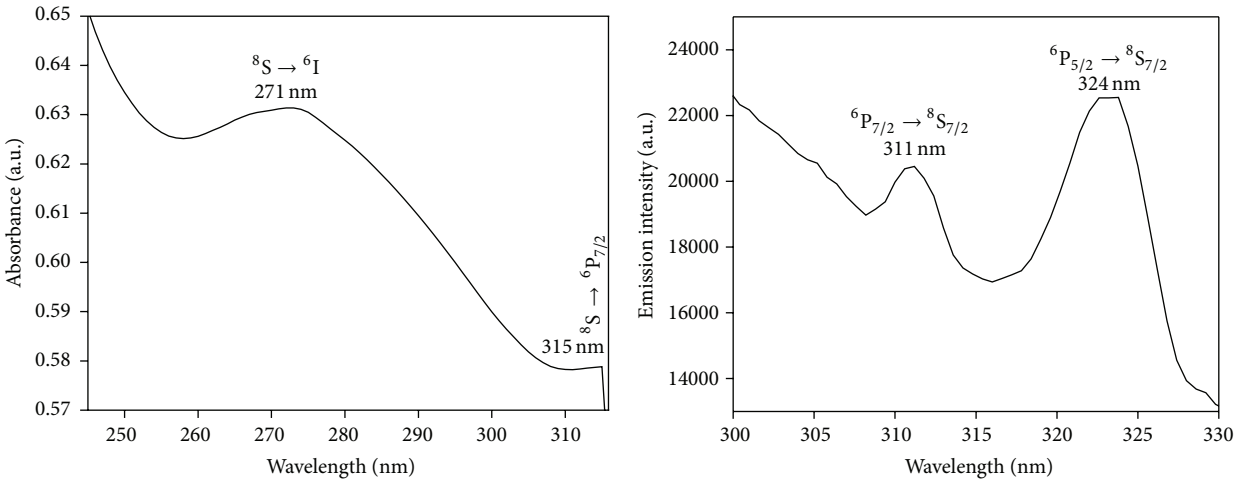

(a) PVA:Gd^{3+} (b) PVA:Gd^{3+}

Figure 3: (a, b) Absorption (a) and (b) emission spectra of PVA:Gd^{3+} polymer films.

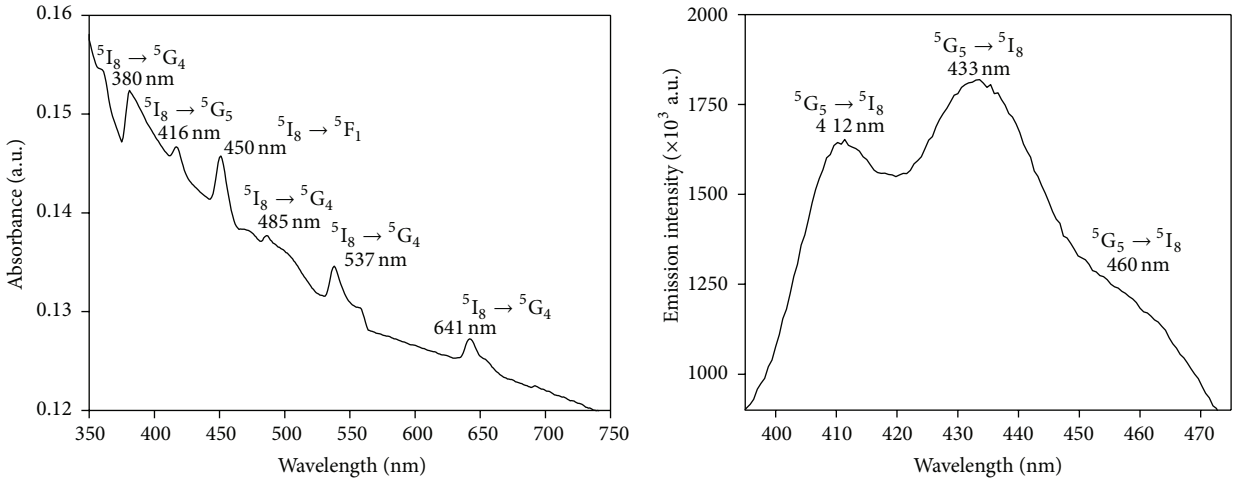

(a) PVA:Ho^{3+} (b) PVA:Ho^{3+}

Figure 4: (a, b) Absorption (a) and emission spectra of PVA:Ho^{3+} polymer films.

Table 2: Dc conductivity values for PVA:Gd^{3+} and PVA:Ho^{3+} polymer films.

Temperature (K)	PVA:Gd^{3+} ($\times 10^{-6}$ S/cm)	PVA:Ho^{3+} ($\times 10^{-6}$ S/cm)
313	1.234	3.173
323	1.465	3.354
333	2.843	3.975
343	4.965	6.453
353	10.563	8.234
363	15.876	10.453
373	26.124	15.543

parallel combination of a capacitor, which is due to the mobile ions inside the polymer matrix. The bulk resistance has been calculated from the low frequency intercept of the semicircle or high frequency intercept of the spike on the real axis. The bulk resistance R_b decreases with increase in temperature. This may be due to increase in the mobile charge carriers with increasing temperature related increase in the amorphousness of the polymer electrolyte, which has been confirmed by XRD analysis [25, 26]. The conductivity increased with increase in temperature but the rate of increase was different in different temperature regions as shown in Table 2. From, Figures 8(a) and 8(b) show a typical $1000/T$ versus $\log(\sigma_{DC})$ plot for Gd^{3+}:PVA and Ho^{3+}:PVA polymer films. From the slopes of these plots, the activation energies were calculated using the Arrhenius relation:

$$\sigma_{DC} = \sigma_o \exp\left[\frac{(-E)}{K_B T}\right], \quad (1)$$

where σ_{DC} is the conductivity at temperature T, σ_o is a constant, E is the activation energy, and K_B is the Boltzmann

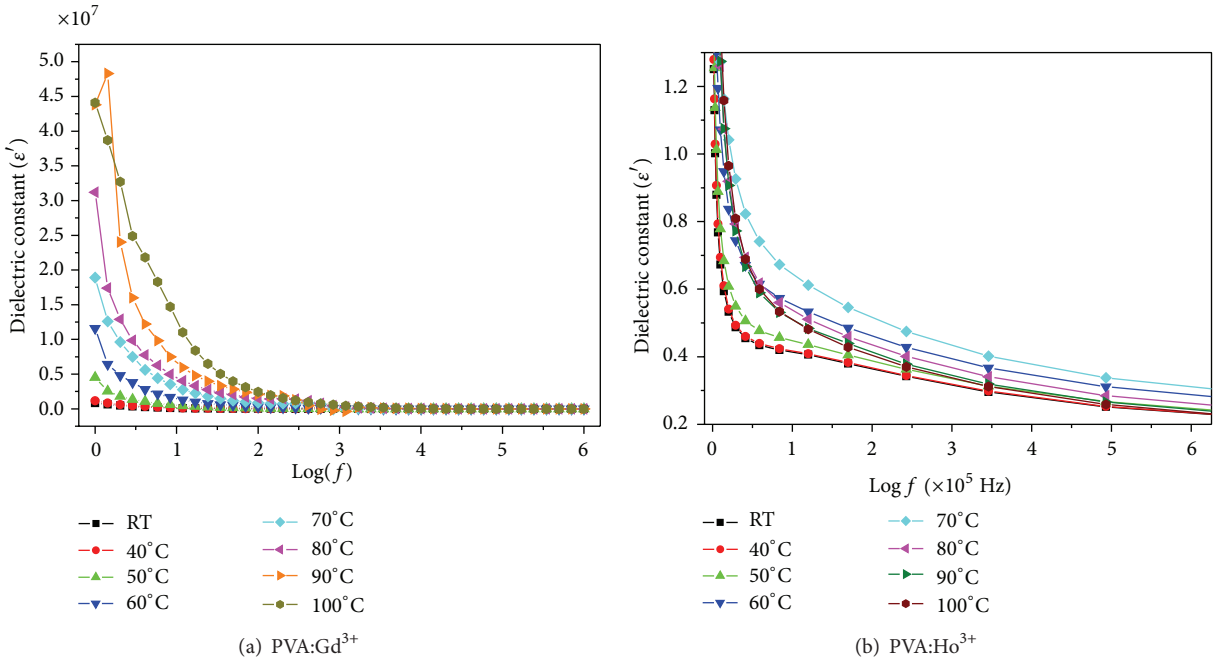

FIGURE 5: (a, b) Dielectric constant varies with frequency for PVA:Gd^{3+} and PVA:Ho^{3+} polymer films.

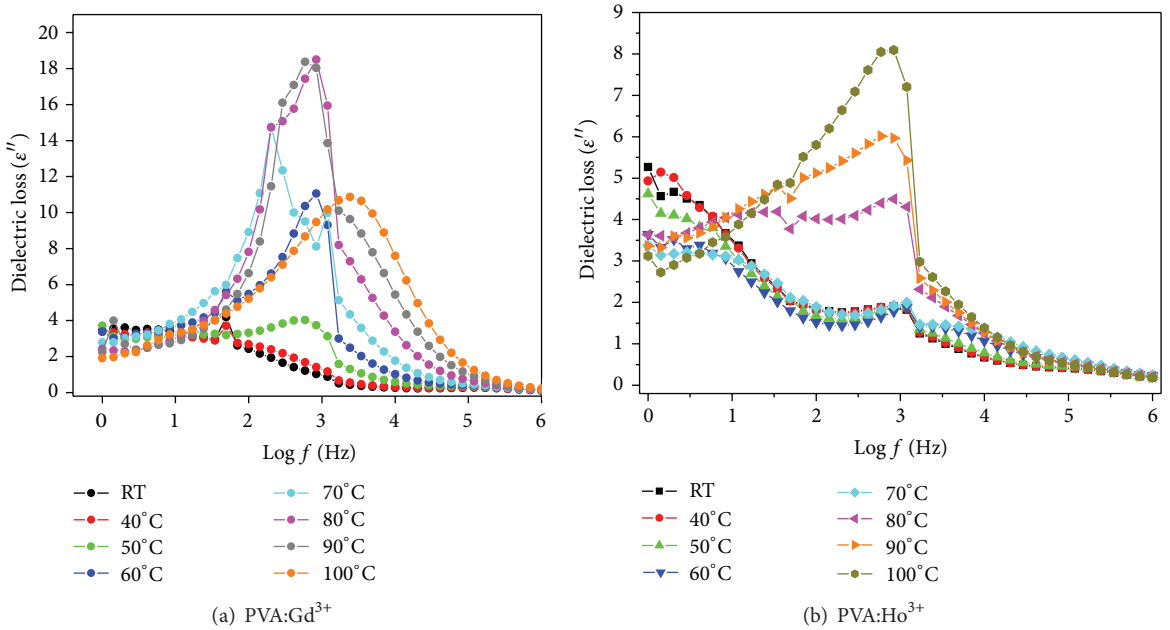

FIGURE 6: (a, b) Dielectric loss varies with frequency for PVA:Gd^{3+} and PVA:Ho^{3+} polymer films.

constant. Arrhenius plots show nonlinearity which suggest that the ion transport in polymer electrolytes depends on the polymer segmental motion [27].

3.6. Magnetic Behavior Analysis. Figure 9(a) shows the measured room temperature magnetization curve for Gd^{3+} doped PVA polymer film, indicating the existence of RT ferromagnetism nature. From the loop coercive field, saturation magnetization (M_s) and remnant magnetization (M_r) were estimated to be 857.59 Oer, 5.75×10^{-3} emu/gm, and 228.42×10^{-6} emu, respectively. This can be explained by RKKY theory; that is, 4f states are highly localized with negligible overlap, and the 4f moments are coupled via RKKY-type exchange, which is mediated by the valence electrons. The 4f moments lead to an induced polarization of the 6s and 5d valence electrons, resulting in a measured magnetic moment.

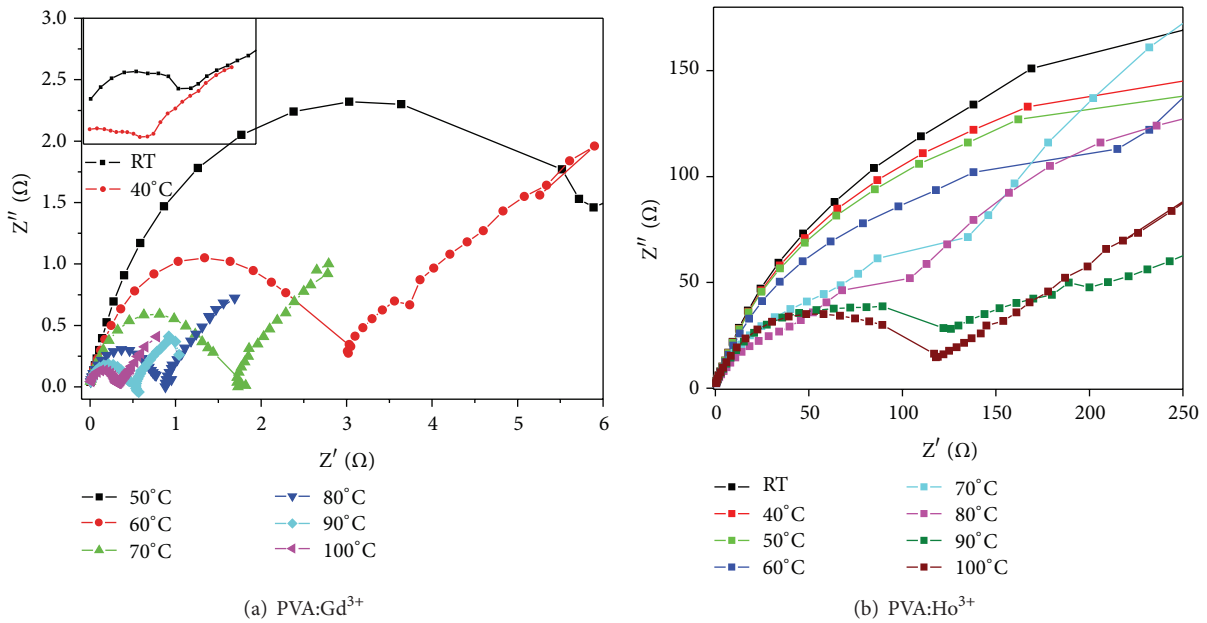

(a) PVA:Gd^{3+} (b) PVA:Ho^{3+}

FIGURE 7: (a, b) Cole-Cole plots for PVA:Gd^{3+} and PVA:Ho^{3+} polymer films.

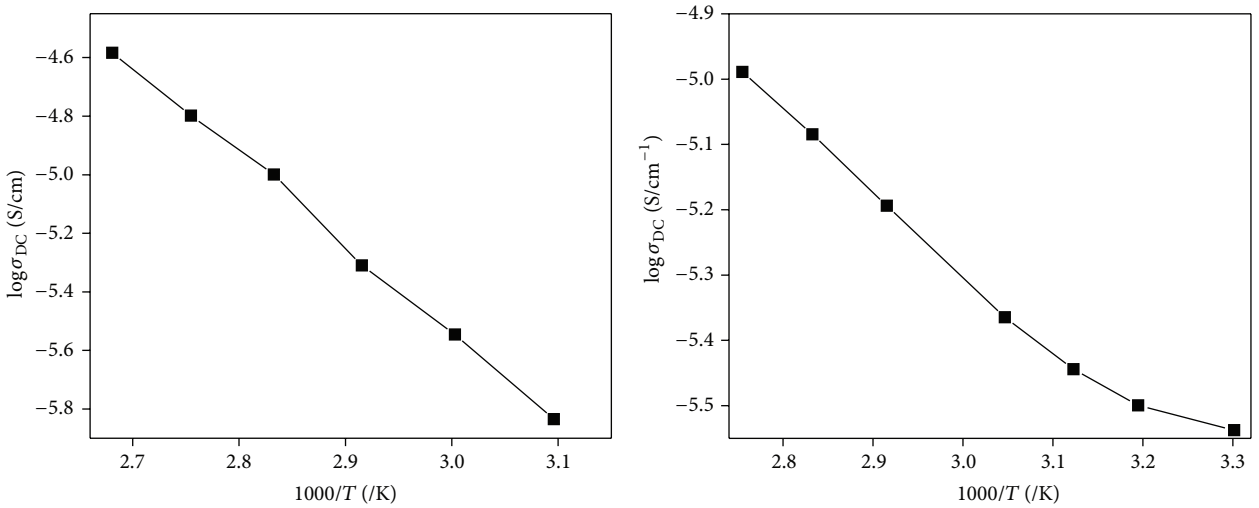

(a) PVA:Gd^{3+} (b) PVA:Ho^{3+}

FIGURE 8: (a, b) Arrhenius plots for PVA:Gd^{3+} and PVA:Ho^{3+} polymer films.

Therefore, it is reasonable to suggest that the observed ferromagnetism is due to oxygen vacancies and/or defects in the polymer film. Figure 9(b) shows the results of PVA:Ho^{3+} polymer film, indicating strong paramagnetic nature. From the loop coercive field, saturation magnetization (M_s) and remnant magnetization (M_r) were estimated to be 41.42 Oer, 11.83 × 10^{-3} emu/gm, and 32.07 × 10^{-6} emu, respectively, which reveals the existence of defects and impurities, and we believe that the observed strong paramagnetism is caused both by the defects (such as oxygen vacancies) and with Ho ions incorporation. From the graphs PVA:Gd^{3+} shows ferromagnetism and PVA:Ho^{3+} shows paramagnetic nature [28, 29].

4. Conclusions

In summary, it could be concluded that we have successfully developed highly transparent and stable Gd^{3+} and Ho^{3+}:PVA polymer films were prepared by solution casting method. The XRD studies reveal the amorphous nature of the polymer that produces greater ionic diffusion. FTIR reveals the complexation between polymer and dopants. The conductivity is found to exhibit increasing trend with increasing temperature. The maximum conductivity of PVA:Gd^{3+} film is 2.621 × 10^{-5} S/cm at 373 K and for PVA:Ho^{3+} film is 15.564 × 10^{-5} S/cm at 353 K. From magnetic profile PVA:Gd^{3+} shows ferromagnetic nature and PVA:Ho^{3+} shows the paramagnetic nature. Hence,

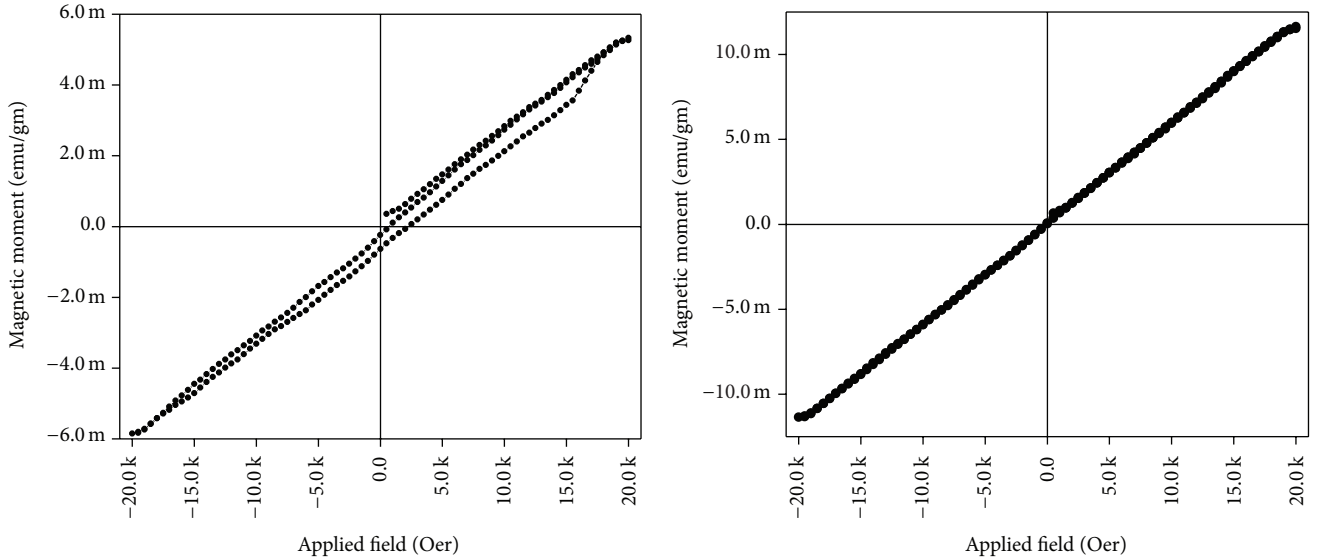

(a) PVA:Gd^{3+} (b) PVA:Ho^{3+}

FIGURE 9: (a, b) Magnetization dependence of the applied field for (a) PVA:Gd^{3+} and (b) PVA:Ho^{3+} polymer films.

these polymer films can be used in electrochemical display systems.

Conflict of Interests

The authors declare that there is no conflict of interests regarding the publication of this paper.

Acknowledgment

The present paper is dedicated to our Research Supervisor Professor (Late) Sri S. Buddhudu Garu for his support and encouragement for all this work.

References

[1] M. Sağlam, M. Biber, A. Türüt, M. S. Ağirtaş, and M. Çakar, "Determination of the characteristic parameters of polyaniline/p-type Si/AI structures from current-voltage measurements," *International Journal of Polymeric Materials*, vol. 54, no. 9, pp. 805–813, 2005.

[2] A. H. Salama, M. Dawy, and A. M. A. Nada, "Studies on dielectric properties and AC-conductivity of cellulose polyvinyl alcohol blends," *Polymer-Plastics Technology and Engineering*, vol. 43, pp. 1067–1083, 2004.

[3] A. Wnuk, M. Kaczkan, Z. Frukacz et al., "Infra-red to visible up-conversion in holmium-doped materials," *Journal of Alloys and Compounds*, vol. 341, no. 1-2, pp. 353–357, 2002.

[4] K. Toyoshima, "Acetalization of polyvinyl alcohol," in *Polyvinyl Alcohol Properties and Applications*, C. A. Finch, Ed., chapter 15, pp. 391–411, John Wiley & Sons, London, UK, 1973.

[5] S. N. Ege, *Organic Chemistry*, The University of Michigan, Ann Arbor, Mich, USA, 1989.

[6] F. Billmeyer Jr., *Text Book of Polymer Science*, Wiley, Singapore, 1984.

[7] G. Hirankumar, S. Selvasekarapandian, N. Kuwata, J. Kawamura, and T. Hattori, "Thermal, electrical and optical studies on the poly(vinyl alcohol) based polymer electrolytes," *Journal of Power Sources*, vol. 144, no. 1, pp. 262–267, 2005.

[8] H. Zhang and J. Wang, "Vibrational spectroscopic study of ionic association in poly(ethylene oxide)-NH_4SCN polymer electrolytes," *Spectrochimica Acta Part A: Molecular and Biomolecular Spectroscopy*, vol. 71, no. 5, pp. 1927–1931, 2009.

[9] S.-K. Jeong, Y.-K. Jo, and N.-J. Jo, "Decoupled ion conduction mechanism of poly(vinyl alcohol) based Mg-conducting solid polymer electrolyte," *Electrochimica Acta*, vol. 52, no. 4, pp. 1549–1555, 2006.

[10] G. Blasse and B. C. Grabmaier, *Luminescent Materials*, Springer, Berlin, Germany, 1994.

[11] S. V. Eliseeva and J. G. Bünzli, "Lanthanide luminescence for functional materials and bio-sciences," *Chemical Society Reviews*, vol. 39, no. 1, pp. 189–227, 2010.

[12] B.-L. An, M.-L. Gong, K.-W. Cheah, W.-K. Wong, and J.-M. Zhang, "Synthesis, structure and photoluminescence of novel lanthanide (Tb(III), Gd(III)) complexes with 6-diphenylamine carbonyl 2-pyridine carboxylate," *Journal of Alloys and Compounds*, vol. 368, no. 1-2, pp. 326–332, 2004.

[13] B. Ding, E. Kimura, T. Sato, S. Fujita, and S. Shiratori, "Fabrication of blend biodegradable nanofibrous nonwoven mats via multi-jet electrospinning," *Polymer*, vol. 45, no. 6, pp. 1895–1902, 2004.

[14] M. Abdelaziz and E. M. Abdelrazek, "Effect of dopant mixture on structural, optical and electron spin resonance properties of polyvinyl alcohol," *Physica B: Condensed Matter*, vol. 390, no. 1-2, pp. 1–9, 2007.

[15] M. Abdelaziz and M. M. Ghannam, "Influence of titanium chloride addition on the optical and dielectric properties of PVA films," *Physica B: Condensed Matter*, vol. 405, no. 3, pp. 958–964, 2010.

[16] M. Krumova, D. López, R. Benavente, C. Mijangos, and J. M. Pereña, "Effect of crosslinking on the mechanical and thermal

properties of poly(vinyl alcohol)," *Polymer*, vol. 41, no. 26, pp. 9265–9272, 2000.

[17] R. Jayasekara, I. Harding, I. Bowater, G. B. Y. Christie, and G. T. Lonergan, "Preparation, surface modification and characterisation of solution cast starch PVA blended films," *Polymer Testing*, vol. 23, no. 1, pp. 17–27, 2004.

[18] G. Kaur, Y. Dwivedi, and S. B. Rai, "Gd^{3+} sensitized enhanced green luminescence in Gd:Tb$(Sal)_3$Phen complex in PVA," *Journal of Fluorescence*, vol. 21, no. 1, pp. 423–432, 2011.

[19] W. van Schaik, M. M. E. van Heek, W. Middel, and G. Blasse, "Luminescence and energy migration in a one-dimensional Gd^{3+} compound: $Ca_4GdO(BO_3)_3$," *Journal of Luminescence*, vol. 63, no. 3, pp. 103–115, 1995.

[20] A. K. Singh, S. B. Rai, and V. B. Singh, "Up-conversions in Ho^{3+} doped tellurite glass," *Journal of Alloys and Compounds*, vol. 403, no. 1-2, pp. 97–103, 2005.

[21] F. S. Liu, Q. L. Liu, J. K. Liang et al., "Optical spectra of Ln^{3+} (Nd^{3+}, Sm^{3+}, Dy^{3+}, Ho^{3+}, Er^{3+})doped Y_3GaO_6," *Journal of Luminescence*, vol. 111, no. 1-2, pp. 61–68, 2005.

[22] L. E. Udrea, D. Hritcu, M. I. Popa, and O. Rotariu, "Preparation and characterization of polyvinyl alcohol—chitosan biocompatible magnetic microparticles," *Journal of Magnetism and Magnetic Materials*, vol. 323, no. 1, pp. 7–13, 2011.

[23] M. Hema, S. Selvasekerapandian, and G. Hirankumar, "Vibrational and impedance spectroscopic analysis of poly(vinyl alcohol)-based solid polymer electrolytes," *Ionics*, vol. 13, no. 6, pp. 483–487, 2007.

[24] L. O. Faria and R. L. Moreira, "Dielectric behavior of P(VDF-TrFE)/PMMA blends," *Journal of Polymer Science Part B: Polymer Physics*, vol. 37, no. 21, pp. 2996–3002, 1999.

[25] R. J. Sengwa and S. Sankhla, "Dielectric dispersion study of poly(vinyl pyrrolidone)-polar solvent solutions in the frequency range 20 Hz-1 MHz," *Journal of Macromolecular Science. Part B: Physics*, vol. 46, no. 4, pp. 717–747, 2007.

[26] S. Rajendran, M. Sivakumar, R. Subadevi, and M. Nirmala, "Characterization of PVA-PVdF based solid polymer blend electrolytes," *Physica B: Condensed Matter*, vol. 348, no. 1–4, pp. 73–78, 2004.

[27] S. Manjunath, K. R. Anilkumar, M. Revanasiddappa, and M. V. N. A. Prasad, "Frequency-dependent conductivity and dielectric permittivity of polyaniline/TiO_2 composites," *Ferroelectrics Letters Section*, vol. 35, no. 1-2, pp. 36–46, 2008.

[28] R. K. Singhal, M. S. Dhawan, S. K. Gaur et al., "Room temperature ferromagnetism in Mn-doped dilute ZnO semiconductor: an electronic structure study using X-ray photoemission," *Journal of Alloys and Compounds*, vol. 477, no. 1-2, pp. 379–385, 2009.

[29] A. Samariya, R. K. Singhal, S. Kumar et al., "Defect-induced reversible ferromagnetism in Fe-doped ZnO semiconductor: an electronic structure and magnetization study," *Materials Chemistry and Physics*, vol. 123, no. 2-3, pp. 678–684, 2010.